2011 IEEE International Conference on Rehabilitation Robotics
Rehab Week Zurich, ETH Zurich Science City, Switzerland, June 29 - July 1, 2011

Development of a Parametric Kinematic Model of the Human Hand and a Novel Robotic Exoskeleton

T. M. W. Burton, R. Vaidyanathan, S. C. Burgess, A. J. Turton and C. Melhuish

Abstract—**This paper reports the integration of a kinematic model of the human hand during cylindrical grasping, with specific focus on the accurate mapping of thumb movement during grasping motions, and a novel, multi-degree-of-freedom assistive exoskeleton mechanism based on this model. The model includes thumb maximum hyper-extension for grasping large objects (~>50mm). The exoskeleton includes a novel four-bar mechanism designed to reproduce natural thumb opposition and a novel synchro-motion pulley mechanism for coordinated finger motion. A computer aided design environment is used to allow the exoskeleton to be rapidly customized to the hand dimensions of a specific patient. Trials comparing the kinematic model to observed data of hand movement show the model to be capable of mapping thumb and finger joint flexion angles during grasping motions. Simulations show the exoskeleton to be capable of reproducing the complex motion of the thumb to oppose the fingers during cylindrical and pinch grip motions.**

I. Introduction

Today, stroke is the single most common cause of severe disabilities in the developed world, with over 130,000 new cases each year in the UK alone [1, 2]. Although the majority of stroke victims survive at least a year, over 1/3 sustain moderate to severe disabilities relating to speech, concentration, cognition or movement [1], including partial or complete motor limitation in the extremities [3, 4, 5].

Hand function is often impaired after stroke [3] and it has been specifically reported [6] that the majority of stroke patients starting rehabilitation face significant impairment of at least one arm, with only 14% actually recovering sensory-motor function. Recent reports have also put forth the premise that arm and hand function are actually more important than mobility for patient independence in everyday life [6] with [7] stating the use of the hand for grasping an object to manipulate it is a critical part of regaining independence.

Work by Napier [8] and Landsmeer [9] on the prehensile movement of the human hand indicates the grasping motions of the hand consists of two basic patterns, power grip and precision grip/handling. All other specialized motions can be derived from these two basic patterns depending on the purpose of the action [8]. Current physio and occupational therapy practices feature the cylindrical and pinch grips heavily during rehabilitation, this reflects their importance as a patients recovery of these motions facilitates a greater level of independence and subsequent quality of life.

Effective post stroke therapy encourages the patient to use the affected limb to complete repetitive, task specific training tasks in order to regain coordinated motor control of the affected area [10]. Robot assisted therapy has been shown to increase the effectiveness of therapy in both the range of motion and the coordinated control of limbs when compared to traditional methods alone e.g. [11, 12]. However, the human hand is a very complex structure consisting of 16 joints with 22 degrees of freedom and is capable of incredibly fine and dexterous movements. This complexity can be seen in figure 1 and makes the design of a rehabilitation device a difficult task. The terms and abbreviations for describing the bones and joints of the hand as used in this paper can be found in [13].

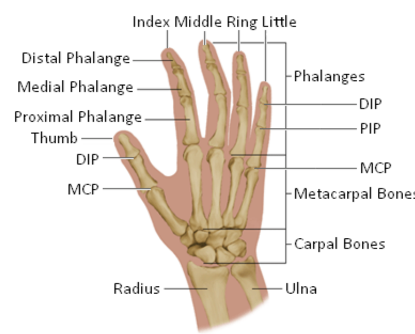

Figure 1. The Human Hand. Modified from [14].

Several devices have been developed with the aim of increasing patient hand function following stroke [1]. While these devices aim to rehabilitate hand function, with the exception of [20] none of the devices listed model the hand as part of there design or operation. Furthermore, many of the devices are bulky being either table mounted or fitted to a robotic manipulator e.g [20]. Everyday grasping function is restricted in [29] by the mechanism occupying the palmer side of the hand preventing objects being grasped. A number of devices e.g. [28, 17, 27] have been designed to fit on the dorsal side of the hand but require adjustment mechanisms to fit different hands which can increases weight. As such it is believed none of the devices fully satisfy the required criteria for being used external to a clinical setting in everyday living.

This work was supported by the University of the West of England, Faculty of Health and Life Sciences under the direction of Dr Kevin Foreman and an EPSRC Doctoral Training Apprenticeship.

Thomas Burton is with the Bristol Robotics Laboratory, University of Bristol and the University of the West of England, Frenchay Campus, BS16 1QD. e-mail: thomas.m.burton@bristol.ac.uk.

Ravi Vaidyanathan is with the Department of Mechanical Engineering, University of Bristol, Queens Building, BS8 1TR and the Department of Systems Engineering at the US Naval Postgraduate School, Monterey, CA, USA, 93940. e-mail: r.vaidyanathan@bristol.ac.uk.

Stuart Burgess is with the Department of Mechanical Engineering, University of Bristol, Queens Building, BS8 1TR. e-mail: s.c.burgess@bristol.ac.uk

[1][11, 15, 16, 17, 18, 19, 20, 21, 22, 23, 24, 25, 26, 27, 28, 29]

978-1-4244-9861-1/11/$26.00 ©2011 IEEE

It is the opinion of the authors that the next logical step in rehabilitation devices for the hand will be to make them useable in everyday situations away from hospital settings and to furthermore have designs specifically tailored to a patients physiology matching the hands natural motion and ability.

Research to date has enabled the calculation of fingertip trajectories, the workspace and kinematics of the hand and the bio-mechanical structure of the hand [2]. Thumb MCP motion to oppose the fingers during grasping for use with a haptic device has been modelled by [37] with [36] modeling thumbtip force via a kinematic description of the thumb. The axis for the thumb MCPs opposition are predicted by [38].

The kinematics developed in the models of [35, 32] used observed motion data from a subject in order to reproduce the trajectory. This work has developed a model that can predict the natural motion for a healthy hand of any size without first having to observe hand motion. This approach was taken by Huang et al [20] who developed a kinematic model of the cylindrical grasp for use in the design and operation of a rehabilitation device. However, their model gave less attention to the motion of the thumb to oppose the fingers.

Cylindrical and pinch grips depend on the abducting and rotation motion of the thumb at the CMC joint to oppose the fingers [8, 39]. In addition the ability to abduct the thumb is essential for shaping the hand during reaching to grasp an object [40]. Weakness and impaired motion of the thumb is often responsible for difficulties experienced [41, 42] and as a consequence training palmer abduction and rotation of the thumb receives particular attention in physical therapy [43].

As the thumb has such an important dynamic role in reach to grasp and in grip formation a device for rehabilitation is required to guide the thumb from its starting neutral position into the opposed position. Hence the modelling of this motion is of significant importance. This work extends the results of [37] by including further anatomical information from [14] to calculate the orientation and trajectory of the joint relative to the finger digits which is then used to optimize a novel mechanism for controlling the motion of the thumb.

The goal of this study was to develop a parameterized kinematic model of the cylindrical grasp by a healthy human hand while using parameters that are readily obtainable from patients such as hand length, breadth and joint thickness. This allows for the trajectory of each joint to be calculated for any size of hand. Knowing the correct trajectory of the hand required for grasping an object, a rehabilitation device will be able to compensate for any deficiencies present in the coordination of the joints that would inhibit successful reach and grasping of an object in everyday living. It is hoped that by aiding in the coordination of the joints for grasping during post stroke therapy, the time taken for a patient to regain successful hand function will be reduced thus increasing a patient's independence and subsequent quality of life. The use of parameterization creates the potential for a device to be manufactured to fit an individual's specific physiological needs maintaining the patient orientated methodology of this project.

[2][30, 14, 31, 20, 32, 33, 34, 35, 36]

II. METHODS

The assumptions regarding the bio-mechanics of the hand and the subsequent kinematic model can be found in [13]. All assumptions are kept constant in this paper with the exception that the distal phalange does not lie perpendicular to the radius of the object as in [13] but is considered to have tip thickness equal to half the DIP thickness shown in figure 3.

A. Thumb Model Assumptions

1) Aligning Thumb Carpal - Metacarpal segments: The model assumes that when the thumb lies in the relaxed position the carpal and metacarpal bones align as shown by figure 2 (A). The approximate CoR (Centre of Rotation) of each of these segments are calculated using the method described by Buchholz et al [14] and further refined by Huang et al [20]. To simplify, the flexion/extension and abduction/adduction axis are assumed to be orthogonal and intersecting contrary to [38].

2) Relaxed and Abducted Angles: The initial orientation of the thumb carpo-metacarpal segment is assumed to lie at 35^0 to the plane of the palm as described by Taylor [34], figure 2 (A). The carpal segment is then assumed to remain fixed in this orientation with the metacarpal segment abducting and rotating such that the angle between the effective segment formed between the wrist CoR and the thumb MCP lies at approximately 50^0 to the plane of the palm as shown by θ_{AB} in figure 4. This value lies within the accepted range of $45^0 - 60^0$ for the abduction angle of the thumb MCP joint [44, 20].

3) Thumb MCP Position During Grasps : It is assumed that when relaxed the thumb MCP joint is orientated such that the palmer side of the joint aligns on a plane perpendicular to the trans radial and palmer planes and located at the radial side of the index finger MCP joint as shown by the dot-dash line in figure 2(B). When opposing the fingers during grasping the centre of the thumb MCP joint is assumed to align on the same plane but located at the centre of the index finger MCP joint as shown by the solid line in figure 2(B).

4) Thumb MCP Rotation : Similar to [32, 34] the model assumes the thumb rotates by 45^0 at the MCP joint as it moves into opposition of the fingers of the hand, figure 2 (B).

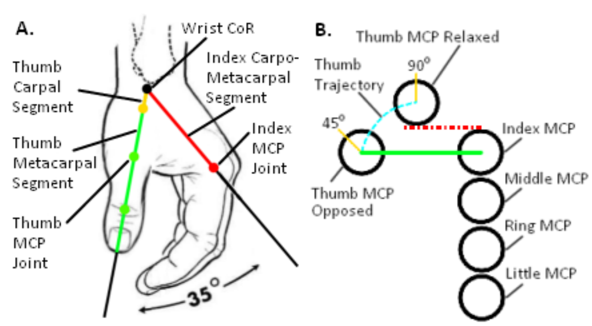

Figure 2. A. The relaxed orientation of the hand with the thumb in the neutral position. B. The MCP joints of the hand as if they were viewed from the trans radial plane at the wrist and the motion of the thumb MCP joint as it rotates from the relaxed position to the opposed position..

5) Shift Between Large and Small Objects : In [13] the thumb MCP and finger MCP joints from base contact points with the object as it is grasped. It was noted that for large objects the thumb reaches maximum hyper-extension and these points shift to the finger MCP and the thumb DIP joints. As the thumb MCP reaches maximum hyper-extension ($\approx -10^0$) it is assumed to lock at this angle with the Wrist CoR to the Thumb DIP considered to be a single segment, figure 3.

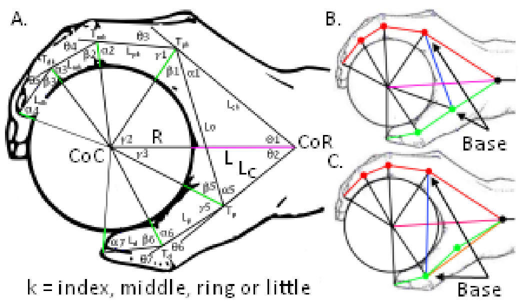

Figure 3. A. Kinematic model of the cylindrical grasp from [13]. B. Small object configuration. C. large object configuration.

The grasping trajectory is constructed by iterating the kinematic model over a range of cylinders encompassing everyday sized objects i.e. drinks cans or hand rails. Humans use visual cues to estimate the size of objects in order to grasp them correctly with the distal joints forming the encompassing shape before the proximal joints rotate the structure to complete the grasp [9]. However, it is believed the aforementioned method will provide greater use in a rehabilitation device where prior knowledge regarding the size of the object is unavailable. By moving the hand along a path of decreasing cylinders it is believed that as contact is made the hand will have the required joint angles to form a successful grasp of the object.

B. Thumb Kinematic Model

Taking into account the assumptions above and in [13] the kinematic model for the rotation and abduction of the thumb to oppose the fingers is shown in figures 4, 5 and 3. Figure 4 shows the thumb as it moves to oppose the fingers for the cylindrical grasp and is described by the equations 1 to 6.

$$\begin{bmatrix} Wx \\ Wy \\ Wz \end{bmatrix} = \begin{bmatrix} 0 \\ 0 \\ 0 \end{bmatrix} \quad (1)$$

$$\begin{bmatrix} X_{F1} \\ Y_{F1} \\ Z_{F1} \end{bmatrix} = \begin{bmatrix} Lci \times \cos(\theta_{CMC}) \\ 0 \\ Lci \times \sin(\theta_{CMC}) \end{bmatrix} \quad (2)$$

$$\begin{bmatrix} X_{T1} \\ Y_{T1} \\ Z_{T1} \end{bmatrix} = \begin{bmatrix} L7 \times \cos(\theta_{REL}) \\ L7 \times \sin(\theta_{REL}) \\ Ct \times \sin(\theta 2) \end{bmatrix} \quad (3)$$

$$\begin{bmatrix} X_{T2} \\ Y_{T2} \\ Z_{T2} \end{bmatrix} = \begin{bmatrix} (L6 + L7) \times \cos(\theta_{REL}) \\ (L6 + L7) \times \sin(\theta_{REL}) \\ Z_{F1} + \frac{Tp}{2} + \frac{Wpk}{2} \end{bmatrix} \quad (4)$$

$$\begin{bmatrix} X_{T3} \\ Y_{T3} \\ Z_{T3} \end{bmatrix} = \begin{bmatrix} L9 \times \cos(\theta_{AB}) \\ L9 \times \sin(\theta_{AB}) \\ Z_{F1} \end{bmatrix} \quad (5)$$

$$\theta 3 = \arctan(\frac{Y_{T3} - Y_{T1}}{X_{T3} - X_{T1}}) \quad (6)$$

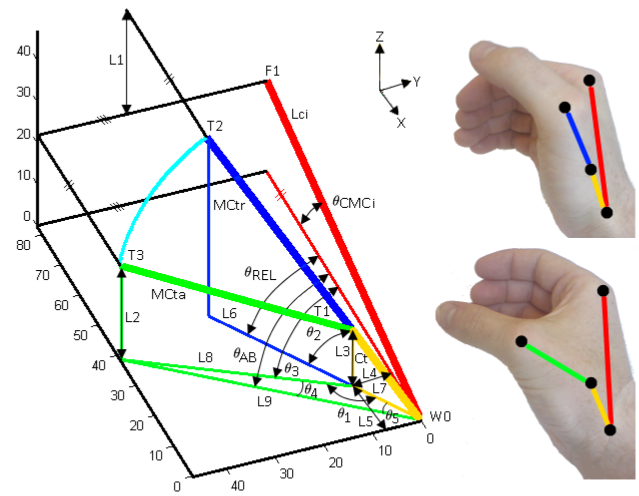

Figure 4. Kinematic model of the thumb. W0, F1, T1, T2 and T3 represent the [x,y,z] coordinates of the Wrist, Index MCP, Thumb Carpal and Thumb MCP joint CoRs in the relaxed and opposed position respectively. Lci is the index CMC length, Ct is the thumb carpal segment length and MCtr and MCta represent the thumb metacarpal segment length in the two positions of relaxed and opposed respectively. The line between T2 and T3 represents the trajectory of the thumb MCP as it moves between the two orientations.

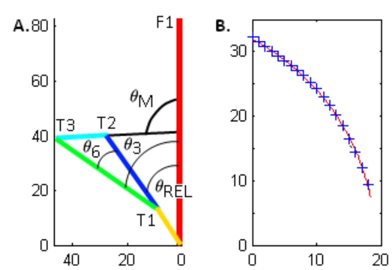

Figure 5. A. Kinematic model of the thumb motion as viewed from above. The line between T2 and T3 shows the angle of the trajectory relative to the index CMC (θ_M). B. MCP motion viewed from the plane of the trajectory.

From figures 4 and 5 equations 7, 8 and 9 can be derived to calculate the angle of the thumb's MCP motion relative to the palmer plane θ_M and the resulting path it follows as shown by the right hand side of figure 5.

$$\theta_M = \arctan(\frac{X_{T3} - X_{T2}}{Y_{T3} - Y_{T2}}) \quad (7)$$

Iterating from $\theta I = \theta 3 \rightarrow \theta REL$ generates the trajectory as shown on the right in figure 5 where Ty is the y value and Tx is the x value as viewed from the plane of the trajectory.

$$T_X = \frac{L8 \times \sin(90 - \theta_M - \theta 3)}{\sin(90 + \theta_M + \theta 3 - \theta I)} \quad (8)$$

$$T_Y = \sqrt{MC_t^2 - T_X{}^2} \quad (9)$$

Figure 4 allows for the orientation and position of the thumb carpal and metacarpal to be calculated when the thumb lies in the opposed position. The two segments can then be described as a single effective carpo-metacarpal segment calculated from parameter $L9$ in figure 4 and shown as Lc in figure 3. With the thumb CMC known, the kinematic model as shown by figure 3 can be used to calculate the joint flexion angles for a range of cylinders. The parameter L is calculated for the index finger

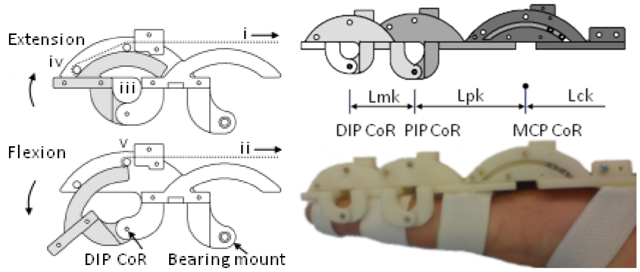

Figure 6. (Left) DIP and PIP bi-directional motion via antagonistic cables and open-pulley configuration. Force applied to cable (i) around the bearing at (iv) produces extension whilst force applied via cable (ii) around bearing (v) results in flexion motion. Spacing at (iii) is set to prevent trapping of the finger joint. (Right) Mechanism CoR axis coincident with finger joint CoR.

and the thumb and kept constant for all other fingers assuming the object's central axis lies perpendicular to the forearm. In addition to the check for large objects a limit is placed on the value of L to prevent it becoming too small which would suggest the object has moved into the hand.

C. Exoskeleton Design

Existing exoskeleton devices do not satisfy all needs of rehabilitation [17]. It is the opinion of the authors that the design requirements for a rehabilitation device should include; A lightweight design to promote greater use, dorsal mounting to allow for tactile feedback during grasping, bi-directional motion to allow for flexion and extension of each joint, kinematics designed to match those of a healthy human hand and the device must be able to deliver key natural hand motions for functional tasks.

The device designed satisfies all of these requirements. Dorsal mounted bi-directional motion is achieved through the use of a novel 'open-pulley' cable drive system. The mechanism is designed parametrically using the kinematic model developed above and in [13] such that the rotational axis of the open-pulley lies coincident to its corresponding hand joint, figure 6. Force transmitted around the joints CoR via the cable and pulley means joint torque is constant throughout the pulleys rotation as described by equation 10. The size of the open-pulley is scaled using a patient's hand dimensions so it has as low a dorsal profile as possible, improving aesthetics and reducing weight. Force transmission to the pulley is via antagonistic Bowden cables manufactured from nylon cable within a PTFE sheath. This configuration yields a lightweight, flexible, low friction force transmission system.

The DIP and PIP joints operate using miniature bearings placed laterally to the joints rotation axis, figure 6. For the MCP joints this is not possible due to the nature of the interaction of the joint within the palm so a slider mechanism similar to [27] is used to create the open-pulley, figure 7.

Actuation for the device comes from braided pneumatic actuators (BPA). BPAs have a high power to weight ratio at the point of application which keeps the weight of the design down. Mounting the BPAs proximally on the forearm close to the elbow lowers the moment arm of the device improving maneuverability for everyday use.

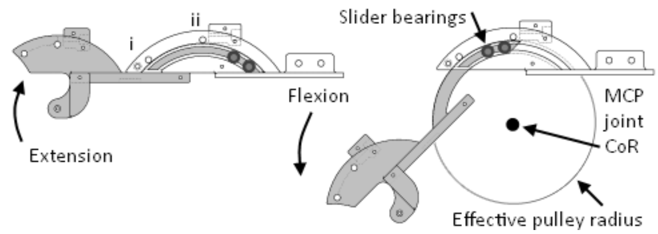

Figure 7. MCP bi-directional motion via antagonistic cables and open-pulley slider configuration. As with the distal joints cables move around distal (i) and proximal (ii) bearings to produce extension and flexion motions.

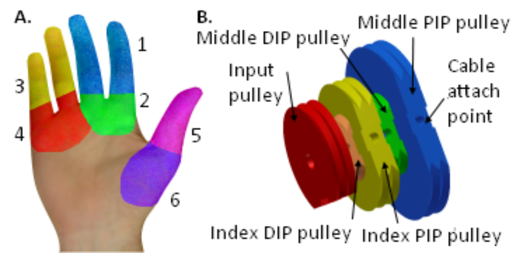

Figure 8. A. Hand functional zones. B. Synchro-motion pulley for zone 1.

The design of the device creates 14 degrees of freedom for the flexion / extension of the finger joints of the hand and thumb. Using 14 BPAs would require a larger number of control valves and a more complex control scheme. The solution was to divide the hand into functional zones and use a synchro-motion pulley mechanism to coordinate the joints within a zone, figure 8. The ratios of the pulleys within a zone are calculated using the kinematic model and the mechanism open-pulley radius of each joint. The zones were chosen so that the maximum number of functional motions could still be achieved while using fewer actuators, for example, changing the ratio of motion between zones 1 and 2 alternates the grasp between pinch and cylindrical. Furthermore the synchro-motion pulleys promote passive self coordination of multiple joints for a patient moving a digit within a functional zone.

For equation 10, K = finger index and J = joint index.

$$\tau_{KJ} = \frac{F_{BPA} \times SPR_I}{OPR_{KJ} \times SPR_{KJ}} - Fr \tag{10}$$

τ_{KJ} = torque at finger joint
F_{BPA} = BPA force
SPR_I = synchro-motion pulley input radius
OPR_{KJ} = open-pulley radius at finger joint
SPR_{KJ} = synchro-motion pulley radius for finger joint
Fr = friction

The opposing motion of the thumb requires a more complex mechanism to match its natural motion. The devices in [20, 24, 22, 27] had mechanisms for controlling motion of the thumb joints however the mechanisms were fixed in one orientation with respect to the fingers. A mechanism for control of the thumb MCP joint to oppose the fingers was proposed in [18] but lacked the model to reproduce natural motion. A novel four bar mechanism has been designed and optimized to match the natural motion of the thumb as described by the kinematic model above, figure 9.

Hard stops are designed into the device to prevent over extension / flexion of any digit.

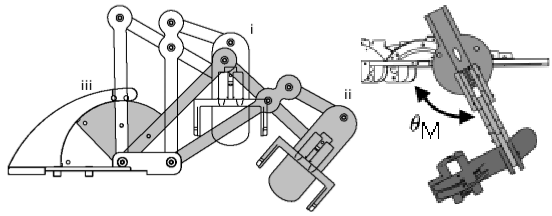

Figure 9. Thumb four bar mechanism optimized to match the natural thumb MCP motion. The mechanism is shown in the orientation of neutral (i) and opposed (ii). The input pulley mechanism is shown by (iii). The angle of the mechanism relative to the plane of the palm is shown on the right.

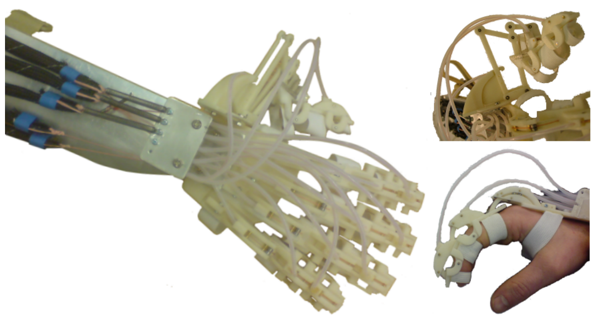

Figure 10. Hand exoskeleton including thumb four bar mechanism (top right) and open pulley system for index finger (bottom right).

D. Testing - Validation

As in [13] the kinematic models accuracy was tested by the direct observation of a subject with healthy hand motion undergoing grasping exercises. Initially the thickness of every joint of a subject's hand was recorded using a modified pair of vernier calipers as shown in figure 11 (C).

The experimental setup consisted of a tripod mounted digital camera (Olympus C480z) orientated with the camera lens parallel to the surface of a worktop, figure 11 (A).

Images were then taken of a single subject's hand at the end of each grasping motion for five different diameter cylinders (41mm, 50.5mm, 66mm, 73.5mm and 89mm) located directly below the camera as shown by figure 11 (B). Markers attached to each joint allowed for surface flexion angles to be measured. The experimental flexion data collected from the subject was fitted with a second order polynomial so that the full natural trajectory range could be plotted and compared against that predicted by the model. A MATLAB script used the kinematic model to generate predicted joint flexion angles for a range of objects (40mm - 90mm radius). The specific values for objects of the same dimensions as those used in the trials were then extracted for comparison, figure 12.

Testing the four bar mechanism for the natural motion of the thumb was conducted in a similar manner. The kinematic model of the thumb motion predicts the angle of the trajectory of the thumb MCP relative to the palmer plane. A camera (Olympus C480z) was orientated as above, figure 11 (A). The subject then rotated the thumb from the relaxed to the abducted opposed position while ten images were taken of the motion. Markers on the thumb MCP joint and the palmer plane allowed for the angle of the motion to be extrapolated and compared to the predicted value. The camera was then orientated towards

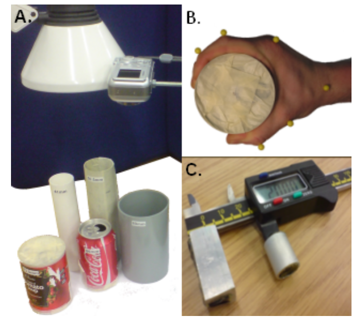

Figure 11. Experimental method for obtaining flexion angles during grasping.

the dorsal side of the thumb MCP joint from the trans radial plane of the wrist at an angle equal to that measured from the previous image data. Nine images were then taken of the thumb as it moved through the predicted arc of motion from relaxed to opposed. As before, a marker on the thumb MCP joint allowed for the motion to be extracted and compared against the models predicted trajectory, figure 13.

The four bar mechanism was synthesised by modelling the kinematics of the mechanism using the link lengths calculated to give the correct start and end positions of the predicted motion of a healthy hand. A MATLAB script was used to generate the trajectory of the mechanism located at the dorsal mid point of the thumb MCP joint so that it could be compared against the predicted and observed trajectory, figure 13.

III. Results

The results here are from a single subject with hand dimensions of 185mm hand length and 90mm hand width.

Figure 12 shows the experimental joint flexion angle data for the index finger against that predicted by the kinematic model. From the specific end point data gathered the average error is 4.28 degrees with a standard deviation of 3.29 degrees across all end points. Figure 12 also shows the data gathered for the thumb flexion angles against those predicted by the kinematic model. For the thumb the average error is 4.82 degrees with a standard deviation of 3.25 degrees. Cumulatively this produces a model error for the index finger and thumb of 4.5 degrees with a 3.27 degree standard deviation. Both the trajectories of the thumb and the index finger have greater accuracy than the results presented in [13].

The error between the predicted MCP trajectory angle (θ_M) and that observed was found to be 1.2 degrees. Figure 13 shows the predicted and observed trajectories of the thumb MCP along the plane formed by angle θ_M. Across each of the nine points identified from the image data the vertical error between the model and the experimental data was found to be 1.2mm with a standard deviation of 0.77mm. The final horizontal error between the end point of the predicted motion and the experimental data is 0.14mm. Figure 13 also shows the trajectory of the synthesised four bar mechanism. The vertical error at the specific points between the mechanism and the predicted motion is 2.66mm with a standard deviation of 1.81mm. The vertical error between the synthesised mechanism and the natural motion of the thumb at the specific points is 3.27mm

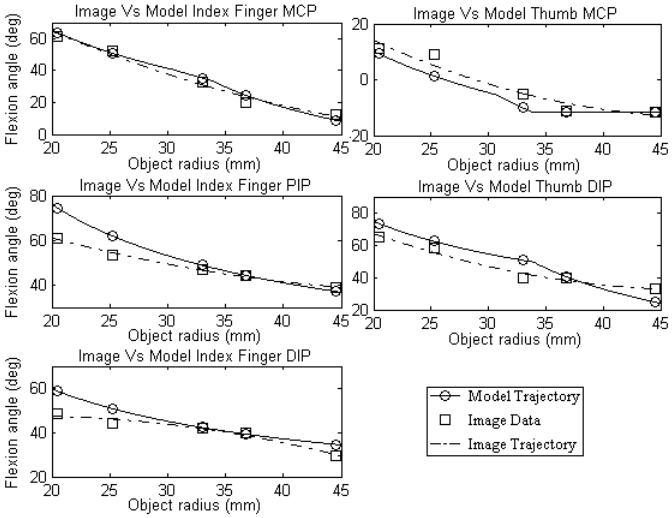

Figure 12. (Left) Index finger surface joint flexion angles. (Right) Thumb surface joint flexion angles.

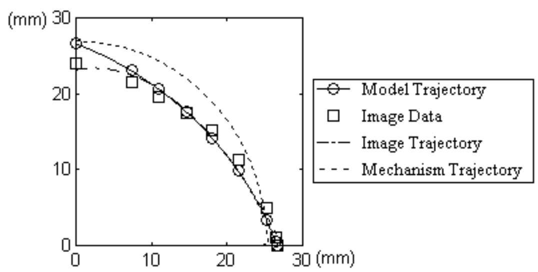

Figure 13. Thumb MCP motion results including four bar synthesis.

with a standard deviation of 1.21mm. The final horizontal error between the mechanism and the predicted motion is 1.22mm and 1.36mm against the natural motion.

IV. Discussion

The hand model presented in [13] had an average finger joint error of 4.6 degrees, the model presented here has made an improvement upon this with an average error of 4.28 degrees but more significantly, the average thumb error in [13] of 13.4 degrees has been reduced to 4.82 degrees. This result suggests the model could be used to predict thumb joint flexion angles. The modelling of the thumb's MCP motion produces promising results with a predicted thumb angle of motion error of 1.2 degrees and an error of 1.2mm in the vertical displacement of the motion along the plane of θ_M. The four bar mechanism for moving the thumb has an error of 3.27mm in vertical displacement so will require further investigation.

While the results presented above are encouraging there is still error within the model and this has been attributed to three mains factors:

1) *Measurement inaccuracies during experimentation* - The method for obtaining joint flexion data as described above allowed for the collection of joint surface angles after post processing of the images, however, it is believed using direct measuring tools such as goniometers may improve the robustness of the data.
2) *Rotation of thumb distal segments* - The thumb distal segments also contain a rotation that was not accounted for within the model. Adding this rotation into the model could further improve the accuracy of the thumb kinematics.
3) *Small objects* - A significant source of error can be seen in the kinematic model for the index finger DIP and PIP joints for small radius objects (~ <25mm radius). In the same way that the model switches base contact points for large objects when the thumb reaches maximum extension it is believed that a second switch for small objects where the base contact points switch to between the thumb MCP and the finger PIP could improve the accuracy. It is believed this is the main reason why the observed flexion angles for small objects are less then those predicted by the model.

V. Conclusion

This work reports the development of a kinematic model of hand motion, with specific focus on the accurate mapping of thumb movement to oppose the fingers during cylindrical and pinch grip motions. These motions have been shown to be of significant importance for normal hand functions and the rehabilitation of hand movement following neurological damage such as stroke [43]. A novel, multi-degree-of-freedom hand exoskeleton has been developed based on parameters from the model and incorporates a four-bar mechanism optimized to fit the thumb motion of the model.

Despite an average joint flexion error of 4.5 degrees it is believed the hand kinematic model presented here shows improvement over previous models. With the significant improvement in thumb joint flexion angle error it is believed that the model has the potential to be used for trajectory planning for a rehabilitation device. However, as stated above, some key improvements will be considered with the aim of improving the accuracy of the model such as a shift in the base contact points for small object (~ <25mm radius) grasping.

The kinematic model of the thumb's motion developed here has been shown to have a high degree of accuracy in prediction the angle of motion and the trajectory of the thumb MCP joint from relaxed to opposed with average errors of 1.2 degrees and 1.2mm in the angle and vertical displacement respectively. The four bar mechanism has been fitted to match the relaxed and opposed orientations of the thumb MCP and while it has been shown to be able to match these configurations the trajectory between the two positions has an error of 3.27mm. Further optimisation of the four bar mechanism will aim to reduce this error so that the trajectory closer matches that of the natural thumb motion. Further experimentation with different subjects will be required to test the scalability of the parametric model.

Using a computer aided design environment a novel hand exoskeleton has been developed that is scaleable to a patient's specific hand physiology. A dorsally mounted, bi-directional, open-pulley mechanism enables the rotation axis of the mechanism to lie coincident with the natural joint CoR. The number of actuators required for functional hand motions has been reduced through the designation of specific functional zones of the hand and the design of a novel synchro-motion pulley system. The exoskeleton design is capable of reproducing the complex motions of the thumb during cylindrical and pinch grip motions as well as a range of digit movements during functional tasks for activities of daily living. A novel four-bar mechanism has been shown to match the start and end points of the thumb MCPs predicted trajectory but will need further refinement to match the natural trajectory closer. Full testing of the joint synchronization will also be required to determine if the design can reproduce the natural motion of the hand when fitted to a person.

REFERENCES

[1] M. R. Laboratories. (1997) Merck manual geriatrics. [Online]. Available: www.merck.com/mrkshared/mmg/home.jsp

[2] R. Tonkin. (2007) Stroke statistics. [Online]. Available: stroke.org

[3] G. Kwakkel, B. J. Kollen, J. van der Grond, and A. J. Prevo, "Probability of regaining dexterity in the flaccid upper limb: Impact of severity of paresis and time since onset in acute stroke," *Stroke*, vol. 34, no. 9, pp. 2181–2186, 2003.

[4] J. T. Khaw, "Epidemiology of stroke," *Journal of neurology, neurosurgery, and psychiatry*, vol. 61, no. 4, pp. 333–338, oct 1996.

[5] P. A. Wolf and J. C. Grotta, "Cerebrovascular disease," *Circulation*, vol. 102, no. 90004, pp. IV–75–80, 2000.

[6] D. Wade. (2000) National clinical guidelines for stroke: London royal college of physicians. [Online]. Available: www.rcplondon.ac.uk/resources/stroke-guidelines

[7] O. Lambercy, L. Dovat, V. Johnson, B. Salman, S. Wong, R. Gassert, T. Milner, T. C. Leong, and E. Burdet, "Development of a robot-assisted rehabilitation therapy to train hand function for activities of daily living," in *Proceedings of the IEEE 10th Intl. Conference on Rehabilitation Robotics (ICORR 2007)*, 2007, pp. 678–682.

[8] J. R. Napier, "The prehensile movements of the human hand," *The Journal of Bone and Joint Surgery*, vol. 38 B, no. 4, pp. 902–913, nov 1956.

[9] J. M. F. Landsmeer, "Power grip and precision handling," *Annals of the Rheumatic Diseases*, vol. 21, no. 2, pp. 164–170, 1962.

[10] H. Woldag and H. Hummelsheim, "Evidence-based physiotherapeutic concepts for improving arm and hand function in stroke patients," *Journal of Neurology*, vol. 249, pp. 518–528, 2002.

[11] C. Takahashi, L. Der-yeghiaian, V. Le, R. Motiwala, and S. Cramer, "Robot-based hand motor therapy after stroke," *Brain*, vol. 131, no. 2, pp. 425–437, 2008.

[12] G. Kwakkel, B. J. Kollen, and H. I. Krebs, "Effects of robot-assisted therapy on upper limb recovery after stroke: A systematic review," *Neurorehabilitation and Neural Repair*, vol. 22, no. 2, pp. 111–121, March/April 2008.

[13] T. Burton, R. Vaidyanathan, S. Burgess, A. Turton, and C. Melhuish, "A parameterized kinematic model of the human hand," in *Proceedings of Towards Autonomous Robotic Systems (TAROS 2010)*, Plymouth, sep 2010, pp. 34–40.

[14] B. Buchholz, T. J. Armstrong, and S. A. Goldstein, "Anthropometric data for describing the kinematics of the human hand," *Ergonomics*, vol. 35, no. 3, pp. 261–273, 1992.

[15] M. Mulas, M. Folgheraiter, and G. Gini, "An emg-controlled exoskeleton for hand rehabilitation," in *International Conference on Rehabilitation Robotics*, 2005, pp. 371–374.

[16] M. Dicicco, L. Lucas, and Y. Matsuoka, "Comparison of two control strategies for a muscle controlled orthotic exoskeleton for the hand," in *The Proceedings of the IEEE International Conference on Robotics and Automation*, 2004, pp. 1622–1627.

[17] A. Wege, K. Kondak, and G. Hommel, "Mechanical design and motion control of a hand exoskeleton for rehabilitation," in *IEEE ICMA*, 2005.

[18] P. Stergiopoulos, P. Fuchs, and C. Laurgeau, "Design of a 2-finger hand exoskeleton for vr grasping simulation," 2003.

[19] Y. Fu, P. Wang, S. Wang, H. Liu, and F. Zhang, "Design and development of a portable exoskeleton based CPM machine for rehabilitation of hand injuries," in *International Conference on Robotics and Biomimetics*, 2007, pp. 1476–1481.

[20] Y. Huang and K. Low, "Initial analysis and design of an assistive rehabilitation hand device with free loading and fingers motion visible to subjects," in *Proceedings of the IEEE International Conference on Systems, Man and Cybernetics (SMC 2008)*, oct 2008, pp. 2584 –2590.

[21] P. Hawkins, J. Smith, S. Alcock, M. Topping, W. Harwin, R. Loureiro, F. Amirabdollahian, J. Brooker, S. Coote, E. Stokes, G. Johnson, P. Mak, C. Collin, and B. Driessen, "Gentle/s project: Design and ergonomics of a stroke rehabilitation system," in *In Proceedings of 1st Cambridge Workshop on Universal Access and Assistive Technology (CWUAAT)*, 2002, pp. 85–90.

[22] R. Loureiro and W. Harwin, "Reach & grasp therapy - design and control of a 9-dof robotic neuro-rehabilitation system," in *International Conference on Rehabilitation Robotics*, 2007, pp. 757–763.

[23] L. Masia, H. Krebs, P. Cappa, and N. Hogan, "Design and characterization of hand module for whole-arm rehabilitation following stroke," in *IEEE/ASME Transactions on Mechatronics*, vol. 12, no. 4, 2007, pp. 399–407.

[24] L. Dovat, O. Lambercy, R. Gassert, T. Maeder, T. M. T. Leong, and E. Burdet, "A cable - actuated rehabilitation system to train hand function after stroke," in *IEEE Transactions on Neural Systems and Rehabilitation Engineering*, vol. 16, no. 6, 2008, pp. 582–591.

[25] C. Marvin. (2007) Portable hand cpm w/soft splint 8091. [Online]. Available: Online

[26] M. Mihelj, J. Podobnik, and M. Munih, "HEnRiE - haptic environment for reaching and grasping exercise," 2008, pp. 907–912.

[27] K. Tong, S. Ho, P. Pang, X. Hu, W. Tam, K. Fung, X. Wei, P. Chen, and M.Chen, "An intention driven hand functions task training robotic system," in *Engineering in Medicine and Biology Society (EMBC), 2010 Annual International Conference of the IEEE*, sep 2010, pp. 3406–3409.

[28] A. Chiri, F. Giovacchini, N. Vitiello, E. Cattin, S. Roccella, F. Vecchi, and M. Carrozza, "Handexos: Towards an exoskeleton device for the rehabilitation of the hand," in *IEEE/RSJ International Conference on Intelligent Robots and Systems 2009 (IROS 2009)*, Oct. 2009, pp. 1106–1111.

[29] M. Bouzit, G. Burdea, G. Popescu, and R. Boian, "The rutgers master ii - new design force-feedback glove," in *IEEE/ASME Transactions on Mechatronics*, vol. 7, no. 2, 2002, pp. 256–263.

[30] N. Brook, J. Mizrahit, M. Shoham, and J. Dayan, "A biomechanical model of index finger dynamics," *Medical Engineering Physics*, vol. 17, pp. 54–63, jan 1995.

[31] D. Dragulescu, V. Perdereau, M. Drouin, L. Ungureanu, and K. Menyhardt, "3D active workspace of human hand anatomical model," *BioMedical Engineering OnLine*, vol. 6, no. 1, p. 15, 2007.

[32] D. G. Kamper, E. G. Cruz, and M. P. Siegel, "Stereotypical fingertip trajectories during grasp," *Journal of Neurophysiology*, pp. 3702–3710, 2003.

[33] S. Parasuraman and K. C. Yee, "Bio-mechanical analysis of human hand," in *Proceedings of the IEEE International Conference on Computer and Automation Engineering*, 2009, pp. 93–97.

[34] C. Taylor and R. J. Schwarz, "The anatomy and mechanics of the human hand," *Artificial limbs*, vol. 2, no. 2, pp. 22–35, 1955.

[35] M. Veber and T. Bajd, "Assessment of human hand kinematics," in *Proceedings of the IEEE International Conference on Robotics and Automation (ICRA 2006)*, may 2006, pp. 2966–2971.

[36] F. J. Valero-Cuevas, M. E. Johanson, and J. D. Towles, "Towards a realistic biomechanical model of the thumb: the choice of kinematic description may be more critical than the solution method or the variability/uncertainty of musculoskeletal parameters," *Journal of Biomechanics*, vol. 36, no. 7, pp. 1019–1030, 2003.

[37] K. Kim, Y. Youm, and W. K. Chung, "Human kinematic factor for haptic manipulation : The wrist to thumb," *HAPTICS*, vol. 20, no. 1, pp. 261–273, 2002.

[38] A. Hollister, W. L. Buford, L. M. Myers, D. J. Giurintano, and A. Novick, "The axes of rotation of the thumb carpometacarpal joint," *Journal of Orthopaedic Research*, vol. 10, no. 3, pp. 454–460, 1992.

[39] M. Nordin and V. H. Frankel, *Basic biomechanics of the musculoskeletal system*. Lippincott Williams I& Wilkins, 2001.

[40] A. M. Wing and C. Fraser, "The contribution of the thumb to reaching movements," *The Quarterly Journal of Experimental Psychology*, vol. 35, pp. 297–309, 1983.

[41] N. Seo, W. Rymer, and D. Kamper, "Altered digit force direction during pinch grip following stroke," *Experimental Brain Research*, vol. 202, pp. 891–901, 2010.

[42] C. E. Lang, S. L. DeJong, and J. A. Beebe, "Recovery of thumb and finger extension and its relation to grasp performance after stroke," *Journal of Neurophysiology*.

[43] J. H. Carr and R. B. Shepherd, *A Motor Relearning Programme for Stroke*, 1987.

[44] L. Y. Chang and Y. Matsuoka, "A kinematic thumb model for the act hand," in *Proceedings of the IEEE Intl. Conference on Robotics and Automation (ICRA '06)*, May 2006, pp. 1000–1005.